Nickel Oxide-Catalyzed Synthesis of 4-Amino-2*H*-Chromenes: Its Application in Antimicrobial Studies and Towards Protein Docking

A. Neela[1], T. Clarina[2,] and V. Rama[2,*,]

[1]Department of Chemistry, Rani Anna Govt. College for Women, Manonmaniam Sundaranar University, Abishekapatti, Tirunelveli-627012, India
[2]Department of Chemistry, Sarah Tucker College, Manonmaniam Sundaranar University, Abishekapatti, Tirunelveli-627012, India

*Corresponding author: E-mail: rama242002@gmail.com

This work involves the synthesis of densely functionalized 2-amino-4*H*-chromenes by domino Knoevenagel-Michael-cyclization reaction of aromatic aldehydes, β-naphthol and malononitrile in the presence of a catalytic amount of a heterogeneous and reusable green NiO nanoparticle at 50 °C. The biogenic nickel oxide nanoparticles are characterized by Fourier transform infrared radiation, X-ray diffraction analysis, scanning electron microscopy and transmission electron microscopy. The synthesized chromenes are characterized by IR, NMR spectra. The synthesized chromene derivatives are studied for microbial inhibition by Kirby-Bauer disc diffusion method using amikacin and flucanazole as positive control. The compounds are found to have good to moderate antimicrobial activities. Their bio evaluation has been carried out with a protein and identified promising ligands for *Mycobacterium tuberculosis* InhA through molecular docking.

Keywords: 2-Amino-4*H*-chromenes, Knoevenagel-Michael cyclization, Antimicrobial activity, Molecular docking.

INTRODUCTION

Green chemistry is increasingly seen as a powerful tool that researchers can use to evaluate the environmental impact of nanotechnology. Here an attempt is made to evaluate the catalytic efficiency of nanoparticles, quantify the greenness of a chemical process and also to factor in new avenues of synergistic chromenes. Chromene derivatives are an important class of heterocyclic compounds, widely distributed in natural products. Chromene and its derivatives have also been recognized as one type of 'privileged medicinal scaffolds' due to their unique pharma-cological and biological activities. Among various chromene family members, 2-amino-4*H*-chromenes are especially important for medicinal applications including anti-microbial [1], antiviral [2], mutagenicity [3], antiprolife-rative [4], antitumor [5], cancer therapy [6] and central nervous system activity [7,8]. This highly potent compound is prepared by multi-component reactions (MCRs) using green NiO nano-particles as an efficient catalyst. In this work, greener ecofriendly process is done by water extract of *Andrographis paniculata* plant. *Andrographis paniculata* contains diterpenes, lactones and flavonoids. Flavonoids mainly exist in the root but have

also been isolated from the leaves. The active ingredients are andrographolide and neoandrographolide, which are derivatives of diterpenoids. Though the main component andrographolide is slightly soluble in water [9], our focus on green synthesis makes us to get water extract just to prepare NiO nanoparticles. The emerging interest to synthesize nanoparticles of nickel oxide is due to its high catalytic efficiency, strong adsorption ability. The synthesis of 2-amino-4*H*-chromenes has already been prepared by heating a mixture of malono-nitrile, aldehyde and activated phenol in the presence of hazardous organic bases such as piperidine [10]. Although different synthetic methods are available to prepare these heterocyclic systems using methane sulphonic acid, preyssler heteropoly acid, ammonium acetate, *N,N*-dimethylamino-functionalized basic ionic liquid, CuSO$_4$·5H$_2$O, DBU, chitosan, *p*-toluene sulfonic acid, Ca(OH)$_2$, nano-magnesium oxide, hexadecyltrimethyl ammonium bromide (HTMAB), polyamine catalyst, 2,2,2-trifluoroethanol, Mg/Al hydrotalcite, microwave-assisted, DBU, PbO, nitriles have been reviewed [11-28]. To the best of our knowledge there is no report in the literature using green NiO nanoparticle as a catalyst for the synthesis of 2-amino-4*H*-chromenes. With increasing emphasis on green chemistry, we wish to report a

facile, three components procedure for the selective synthesis of 2-amino-4*H*-chromenes using different aromatic aldehydes, β-naphthol and malononitrile at 50 °C in the presence of green NiO nanoparticles under stirring conditions. Encouraged by the results, aromatic aldehydes (**1a-j**) bearing both electron-withdrawing and electron donating groups are subjected to three component condensation reaction to give 2-amino-4*H*-chromene derivatives (**4a-j**) under optimized reaction condition (15 mg NiO, 50 °C). Further, antimicrobial screening of these synthesized compounds is done against some bacterial (Gram-positive as well as Gram-negative) and fungal strains. *Mycobacterium tuberculosis* contains unique signature fatty acids, the mycolic acids, that are unusually long chain α-alkyl, β-hydroxy fatty acids of 60-90 carbons encoded by the Mycobacterium gene InhA is a key catalyst in mycolic acid biosynthesis. Studies over the years have established that InhA is the primary molecular target for the past 40 years. Considering the possible application in biomedical fields, protein docking has also been studied using Auto dock 4.2 software package.

EXPERIMENTAL

All chemicals and reagents are purchased from Merck and Aldrich and used without further purification. Melting points are determined with an Electrothermal 9100 melting point apparatus and are uncorrected. FT-IR spectrum is recorded on Shimadzu FT-IR 8300 series instrument in the range of 4000-400 cm^{-1} using potassium bromide pellets. The phase identity and crystalline size of NiO nanoparticles are characterized by Shimadzu X-ray diffractometer (PXRD-7000) using Cu-Kα-radiation of wavelength λ = 1.5406 Å. Morphological features are studied using Hitachi-7000 scanning electron microscopy and transmission electron microscopy. ^{1}H NMR and ^{13}C NMR spectra (400MHz,100MHz) are recorded on a DRX-500 Advance Bruker spectrometer. The percentage of C, H, N in an organic compound is analyzed using the instrument Elemental Vario EL III over a wide range of concentration. The pharmacological activities against a few selected microbial strains are tested by using Kirby-Bauer Disc Diffusion method. The prediction of ligand with minimum energy to target protein is done by Auto dock 4.2 software package. The 3D pose of bound ligand is visualized using different visualizing tools like pymol, pyrx, which can infer the best fit of ligand.

Preparation of extract and synthesis of NiO nanoparticles: Fresh leaves of *Andrographis paniculata* are collected washed in running tap water and shade dried at room temperature. Dried leaves are powdered using a mixer mechanically, sieved and subjected to Soxhlet extraction using deionized water for 2 h. The aqueous solution obtained after extraction is subjected to concentration under reduced pressure at 40 ± 5 °C by rotary flash evaporator. To illuminate the effects of the plant extract, different concentrations (5, 10, 15 and 20 mL) are used by keeping the source of nickel nitrate at a constant value. In this work, the reaction mixture is prepared by adding 15 mL of the plant extract (fuel) and nickel nitrate (0.1 g) as a source of nickel under constant stirring until the colour changes to black. Then it is kept in a preheated muffle furnace maintained at 400 ± 10 °C. NiO nanoparticles are formed after 3 h. The obtained product of NiO nanoparticle is stored in airtight container for further analysis.

General procedure for the synthesis of 2-amino-4*H*-chromenes: A stoichiometric mixture of an aryl aldehyde (1.0 mmol), malononitrile (1.0 mmol), β-naphthol (1.0 mmol), NiO (15 mg) and water (15 mL) as a solvent taken in a round bottom flask, ball-milled for 30 min at 50 °C and then dried in an air oven at 125 °C. The progress of the reaction is monitored by TLC (ethyl acetate:*n*-hexane). Upon completion of the reaction, the product is washed in hot water and purified by recrystallization with hot ethanol. The scheme for the multi-component reaction involving condensation of aromatic alde-hyde (1), malononitrile (2) and the nucleophilic attack of the phenolic -OH from naphthol (3) to the CN moiety to afford 2-amino-4*H*-chromenes is given in **Scheme-I**.
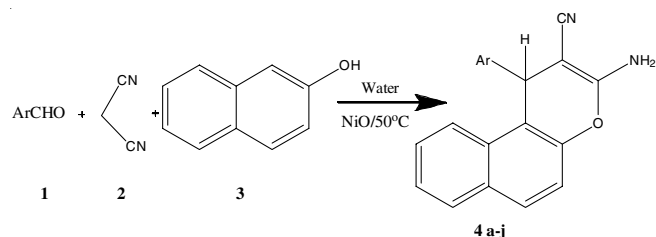
Scheme-I: Synthesis of 2-amino-4*H*-chromenes catalyzed by NiO nanoparticles

Antibacterial assay: The synthesized compounds are evaluated for their *in vitro* antibacterial activity against Gram-negative bacteria such as *Escherichia coli, Klebsiella pneumonia, Pseudomonas aerugenisa, proteus mirabilis* and Gram-positive bacteria *Staphylococcus aureus*. They are also evaluated for their *in vitro* antifungal activity against *Candida albicans* and *Aspergillus oryzae*. Amikacin and flucanazole are used as refere-nces to evaluate the potency of the compounds using Kirby-Bauer disc-diffusion method. Most importantly, this method undoubtedly permits the rapid and quick determination of the efficiency of a drug by measuring diameter of the zones of inhibition that result from diffusion of the agent into soaked-in concentration of various products that can prevent the growth of bacteria and then kept on the surface of the agar plates that have been seeded with organism to be tested [29,30]. The plates are transferred to a box like machine incubator at 37 °C for approximately 10-20 min and allowed to dry and then placing the developed mixture on the agar surface. The plates with the help of a cotton swab are then inoculated with inoculums in order to ensure the full growth and development of the organism. As well-spaced intervals, the discs are transferred to the surface of the agar plates, after incubation, the plates are carefully examined with the growth inhibition, which is indicated by the clear and a vivid zone around each disc. The size of the zone determines the susceptibility of an organism to the drug.

Docking studies: For docking study, we have used Auto dock 4.2 docking software. The structures of the synthesized chromenes are drawn using Chem draw and are converted into their respective pdb format. Molecules are then saved in pdb format and are used as output file for Docking. A protein structure (PDB ID:2NSD) is retrieved from Protein Data Bank using RCSB PDB and is optimized by removing water mole-

cules, residues and hydrogens are added. The minimized structure is used as the receptor protein for docking [31].

RESULTS AND DISCUSSION

Phytochemical screening: The leaf extract of the plant *Andrographis paniculata* is screened for the presence of phytochemical constituents using various tests and the results are recorded in Table-1.

TABLE-1
PHYTOCHEMICAL SCREENING OF LEAF EXTRACT

Compound tested	Test	Inference
Alkaloids	Dragendorffs reagent	–
Tannins	Ferric chloride test	–
Flavonoids	Shibata's reaction	+
Cyanogenic glycosides	Hydrogen cyanide	+
Reducing sugar	Fehling's test	+
Terpenoid	Salkowski test	+

FT-IR analysis: The NiO nanoparticles are synthesized in green and environmentally friendly *via* a simple precipitation method using leaf extract of *Andrographis paniculata* and nickel nitrate as fuel are characterized by various analytical methods. FT-IR spectrum of biosynthesized NiO nanoparticles was recorded to identify the capping and efficient stabilization of the metal nanoparticles by biomolecules present in leaf extract. The peak at 417 cm^{-1} belongs to (Ni---O) stretching frequency [32,33]. The peak at 3516 cm^{-1} corresponds to alcohols and phenols. A second typical absorption peak at 2359 cm^{-1} corresponds to the presence of C=C from the aromatic rings and alkyne bonds in the biomolecules and the observed peak at 1383 cm^{-1} is assigned to germinal methyl. These peaks denote stretching vibrational bands responsible for compounds like flavonoids and terpenoids and so may be held responsible for efficient capping and stabilization of obtained NiO nanoparticles [34,35,40].

From the analysis of FT-IR studies, we confirmed that phenolic compounds have the stronger ability to bind metal indicating that could possibly form the metal nanoparticles to prevent agglomeration and thereby stabilized the medium. This suggests that the biological molecules could possibly perform dual functions of formation and stabilization of NiO nanoparticles in an aqueous medium.

EDAX: The energy dispersive analysis (Fig. 1) indicates how the concentration of elements Ni, O and C varies periodically along the size of atoms being accompanied with maxima of Ni along 52 %, O along 41 %, C along 7 % of distributions and there is no evidence of impurity in the composition.

The purity and crystallinity of synthesized NiO nanoparticles are examined using powder X-ray diffraction as shown in Fig. 2. The peaks positions appearing at 37.5, 43.60, 63.1, 75.7 and 79.7 can be readily indexed as (111), (200), (220), (311) and (222) crystal planes of the bulk NiO, respectively. The XRD pattern shows that the samples are single phase and no other impurities are detected in the distinct diffraction peak except the characteristic peaks of face-centered cubic phase NiO is detected. This result shows that the physical phases of the NiO nanoparticles have higher purity prepared in this work. The NiO lattice constant calculated from the XRD data is 4.1480 Å. The obtained data is matched with the JCPDS file no 471049.
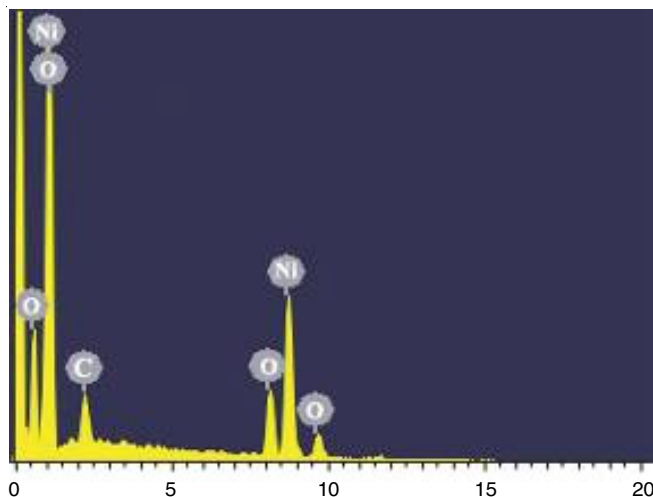

Fig. 1. EDAX of NiO nanoparticles

The particle size is calculated from X-ray diffraction images of NiO powders using Scherrer's formula [36] D = kλ/β cos θ where, K is dimensionless number, which is equal to 0.89, λ is the X-ray wavelength (1.5406 Å for Cu Kα1) employed and β is full width at half maximum of a diffraction peak (FWHM) and θ is the diffraction angle. The value of β is calculated from the following relation, β2 = βs2 – βo2. where, βs is the measured line width at half maximum and β is the instrumental broadening βo = 0.16 with the apparatus used. Crystalline diameter is deduced for the greatest peak magnitude of (2 0 0) through Scherrer's equation. D = 0.89 λ/β cos θ and found as 8.5 nm. X-ray diffraction patterns with no notable diffraction peaks aside from the typical peaks facilitated by the FCC phase NiO nanoparticles with exceptional purity.
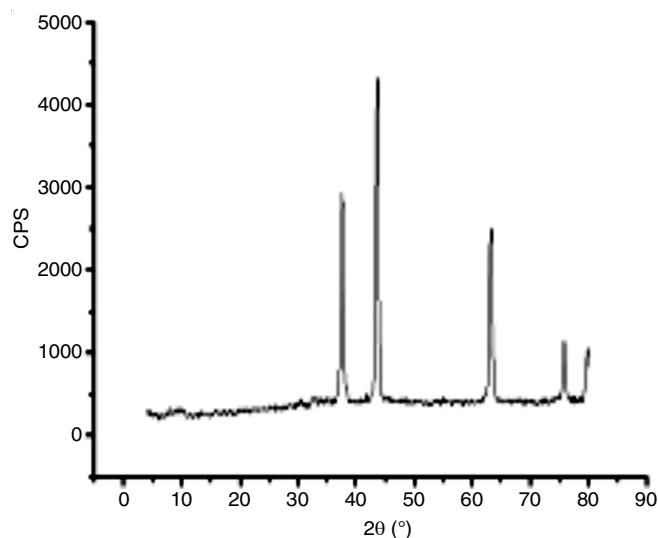

Fig. 2. XRD images of NiO nanoparticles

The sharpness and the intensity of the peaks are quite an indication of the well crystalline nature of the prepared nanoparticles. Specific surface area has a particular importance in case of adsorption, heterogeneous catalysis and reactions on surfaces.

Calculation of specific surface area: The specific surface area can be calculated by:

$$SSA = \frac{6000}{Density\ of\ the\ particle \times D} \quad (1)$$

where D is the size of the particles. The density of NiO is 6.68 g/cm³ and the size obtained from XRD study is 8.5 nm thus the calculated value of the synthesized material NiO is 10567 m²/g. The surface of the synthesized materials is found to be very large and hence the heterogeneous catalytic property is in positive response.

SEM analysis: The surface features of the green synthesized NiO nanoparticles are clearly examined through a scanning electron microscope. The SEM micrographs (Fig. 3a,b) are recorded at magnifications of 20,000x and 50,000x. From the micrographs, it is suggested that the particles are polydispersity and are mostly spherical in shape.
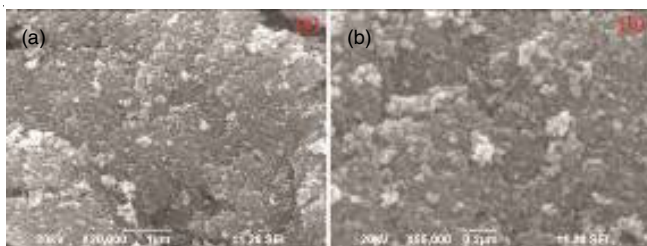

Fig. 3. SEM images of NiO nanoparticles

A few agglomerated nanoparticles are also observed in some places, thereby indicating possible sedimentation at a later time. The biological molecules could possibly perform dual functions of formation and stabilization of NiO nanoparticles in the aqueous medium. The fine particle size results in a large surface area that in turn, enhances the catalytic activity of nanoparticles.

TEM analysis: TEM images of the prepared NiO nanoparticle samples are shown in Fig. 4a,b. It can be seen that the NiO particles have nearly spherical shapes with weak agglomeration. Fig. 4c,d show the corresponding selected area electron diffraction pattern and its Histogram. The SAED pattern consists of five diffraction rings with different radii and one centre. The diameter of the diffraction ring in SAED pattern is proportional to $(h^2 + k^2 + l^2)1/2$, where h, k, l are the Miller indices of the planes corresponding to the ring, counting from the centre 1st, 2nd, 3rd, 4th and 5th rings correspond to (111), (200), (220), (311) and (222) planes, respectively. Tropism of the particles at random and small particles cause the widening of diffraction rings that made up of many diffraction spots, which indicate that the nanoparticles are polycrystalline structure.

The SAED pattern also confirms that the NiO nanoparticles are face-centered cubic, which is consistent with the above XRD results. The Histogram is drawn using MATLAB software on SAED pattern. This gives a number of particles distributed with respect to its size. A maximum number of particles are in the range of 5 to 12 nm. This is reasonably good concurrent with the corresponding parameter of XRD calculations obtained from Debye-Scherer equation.

Preparation of 2-amino- 4*H*-chromenes catalyzed by green NiO nanoparticles: A plausible reaction mechanism for the synthesis of 2-amino-4*H*-chromenes is outlined in **Scheme-II**. At first, aldehyde (1) is activated by NiO catalyst
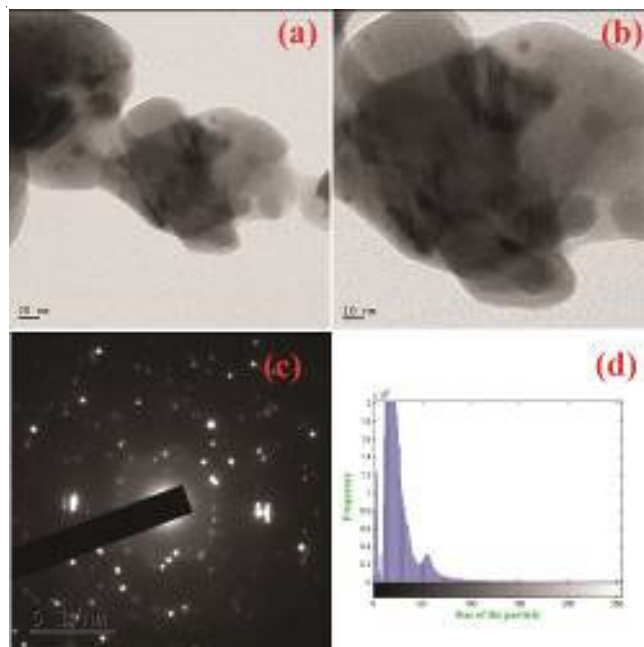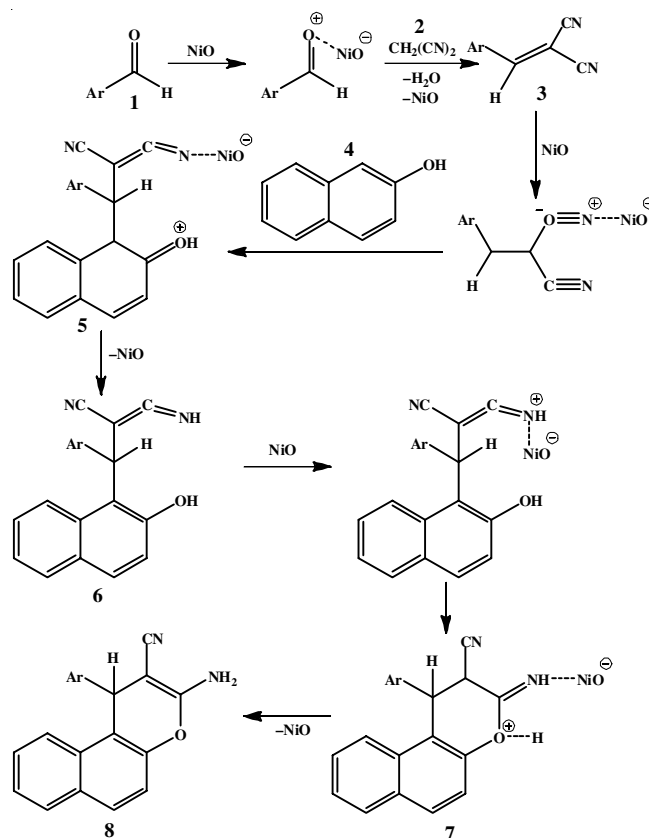

Fig. 4. a, b TEM images of NiO nanoparticles, c, d-SAED pattern & its Histogram

Scheme-II: A plausible reaction mechanism for the synthesis of 2-amino-4*H*-chromenes

to generate 2-arylidenemalononitrile (3), which is formed by Knoevenagel condensation of an activated aldehyde with malononitrile (2). 2-arylidenemalononitrile after activation with NiO has undergone nucleophilic attack by β-naphthol (4) to generate activated intermediate (5), which is simultaneously aromatized (6), activated, undergoes Michael cyclization (7) and NiO is recovered to give the product (8).

Initially, the efforts are focused on the evaluation of varying parameters such as solvent and a catalytic amount of the catalyst on the rate and the yields of obtained 2-amino-4H-chromenes by reacting β-naphthol, aryl aldehydes and malononitrile from the principles of green chemistry point of view.

The results in Table-2 suggest that water is the best solvent in terms of yield and reaction time. In order to examine the catalytic activity of NiO nanoparticles for the preparation of chromenes a mixture of benzaldehyde (1 mmol), malononitrile (1 mmol) and β-naphthol (1 mmol) is stirred in water. Optimization is carried out with variation in the reaction temperature and catalyst amount. No product is observed at room temperature. As the temperature is increased to 50 °C the conversion rate increased as well. From the optimization using a various amount of catalyst loading, it is found that the optimal catalyst amount is 15 mg (Table-3).

TABLE-2
EFFECT OF THE SOLVENT ON THE YIELD, REACTION TIME AND YIELD

Solvent	Time (h)	Yield (%)*
Free	3	80
Water	0.5	98
Ethanol	3	88
Water/ethanol (1:2)	2	70
n-Hexane	6.5	83
CH₂Cl₂	24	60
DMSO	10	20

TABLE-3
OPTIMIZATION OF REACTION CONDITION

Catalyst (mg)	Temp. (°C)	Yield (%)
5	25	60
10	50	70
15	50	89

Following this, a series of 2-amino-4H-chromenes have been synthesized at 50 °C in the presence of a catalytic amount (15 mg) of NiO nanoparticle via one-pot three-component reactions of malononitrile, aromatic aldehydes and β-naphthol. The synergistic effects of multicomponent reactions have been successfully demonstrated to offer an easy way for the synthesis of these compounds in excellent yields. In the scope and limitations of this procedure, a series of experiments is carried out using a variety of aromatic aldehydes (Table-4).

Spectral data

2-Amino-4-phenyl-4H-chromene-3-carbonitrile (4a): White powder, FT-IR (KBr, ν_{max}, cm^{-1}): 3430 (NH₂), 2223 (CN), 1686 (C=C), 1590 (C-O); ¹H NMR (DMSO-d_6, 400 MHz), δ_H (ppm) 8.5 (s, 2H, NH₂), 7.64-7.6 (m, 3H, ArH), 7.94-7.96 (d, 1H, ArH). Elemental analysis: Calculated (%) for C₂₀H₁₄N₂O (298.34): C, 80.51; H, 4.7; N, 9.3. Found: C, 80.32; H, 4.24; N, 8.46.

2-Amino-4-(4-hydroxyphenyl)-4H-chromene-3-carbonitrile (4b): White powder, FT-IR (KBr, ν_{max}, cm^{-1}): 3459 (NH₂, OH), 3346 (CH), 2189 (CN), 1639 (C=C), 1593 (C-O); ¹H NMR (DMSO-d_6, 400 MHz), δ (ppm): 7.6 (d, 1H, ArH) 7-7.4 (m, 3H) 9.7 (s, 2H, NH₂). Elemental analysis: Calculated (%) for C₂₀H₁₄N₂O₂ (314.34): C, 76.41; H, 4.4; N, 8.9. Found: C, 76.30; H, 4.0; N, 8.9.

2-Amino-4-(3-hydroxyphenyl)-4H-chromene-3-carbonitrile (4c): White powder, FT-IR (KBr, ν_{max}, cm^{-1}): 3431 (NH₂, OH), 3337 (CH), 2205 (CN), 1665 (C=C), 1590 (C-O); ¹H NMR (DMSO-d_6, 400 MHz), δ (ppm): 9.5 (s, 1H, OH), 7.06-7.27 (m, 5H), 5.07 (s, 1H, H-4); Elemental analysis: Calculated (%) for C₂₀H₁₄N₂O₂ (314.34): C, 76.41; H, 4.4; N, 8.9. Found: C, 76.26; H, 4.0; N, 8.6.

2-Amino-4-(2-hydroxyphenyl)-4H-chromene-3-carbonitrile (4d): Yellow powder, FT-IR (KBr, ν_{max}, cm^{-1}): 3456 (NH₂, OH), 3334 (NH₂), 2194 (CN), 1641 (C=C), 1573 (C-O); ¹H NMR (DMSO-d_6, 400 MHz), δ (ppm): 8.3 (s, 1H), 7.4 (s, 2H, NH₂), 7.57-7.59 (m, 3H, ArH), 6.63 (s, 2H, ArH). Elemental analysis: Calculated (%) for C₂₀H₁₄N₂O₂ (314.34): C, 76.41; H, 4.4; N, 8.9. Found: C, 76.38; H, 4.3; N, 8.7.

2-Amino-4-(4-nitrophenyl)-4H-chromene-3-carbonitrile (4e): Brown powder, FT-IR (KBr, ν_{max}, cm^{-1}): 3339 (NH₂), 2190 (CN), 1635 (CO), 1585 (C=C), 1251 (C-O), 1379 (NO₂)'; ¹H NMR (DMSO-d_6, 400 MHz), δ (ppm): 8.85 (s, 1H), 7.07 (t, J ¼ 8 HZ, 1H), 6.67–6.64 (m, 3H), 5.74 (s, 2H), 4.31 (s, 1H), 4.05–4.02 (m, 2H), 2.35 (s, 3H), 1.13 (t, 3H) Elemental analysis: Calculated (%) for C₂₀H₁₃N₃O₃ (343.33): C, 69.95; H, 3.8; N, 12.2. Found: C, 69.9; H, 3.6; N, 12.1.

2-Amino-4-(2-nitrophenyl)-4H-chromene-3-carbonitrile (4f): Brown powder, FT-IR (KBr, ν_{max}, cm^{-1}): 3328 (NH₂), 2202 (CN), 1693 (CO); 1369 (NO₂); ¹H NMR (DMSO-d_6, 400 MHz), δ (ppm): d 8.85 (s, 1H), 7.07 (t, 1H), 6.67–6.64 (m, 3H), 5.74 (s, 2H), 4.31 (s, 1H), 4.05–4.02 (m, 2H), 2.35 (s, 3H), 1.13 (t, 3H). Elemental analysis: Calculated (%) for C₂₀H₁₃N₃O₃ (343.33): C, 69.95; H, 3.8; N, 12.2. Found: C, 69.9; H, 3.7; N, 12.3.

TABLE-4
PREPARATION OF 2-AMINO-4H-CHROMENES

Ar	Phenol	Product	Time (min)	Yield (%)	m.p. found (°C)	m.p. reported
C₆H₅	β-Naphthol	**4a**	30	99	273-275	(278-279) [37]
4-OH C₆H₄	β-Naphthol	**4b**	50	76	274-277	(280-282) [37]
3-OH C₆H₄	β-Naphthol	**4c**	60	82	228-230	(225-227) [37]
2-OH C₆H₄	β-Naphthol	**4d**	60	88	254-256	(259-261) [37]
4-NO₂ C₆H₄	β-Naphthol	**4e**	60	91	185-186	(187-188) [37]
2-NO₂ C₆H₄	β-Naphthol	**4f**	50	89	260-262	(262-268) [37]
C₄H₃S	β-Naphthol	**4g**	50	87	244-246	(240-243) [38]
C₅H₄N	β-Naphthol	**4h**	60	82	221-223	(224-226) [38]
C₄H₃O	β-Naphthol	**4i**	50	86	240-244	(246-248) [38]
5-Br-OHC₆H₃	β-Naphthol	**4j**	60	89	272-274	This work

2-Amino-4-(thionyl)-4H-chromene-3-carbonitrile (4g): Yellow powder, FT-IR (KBr, ν_{max}, cm^{-1}): 3422 (NH$_2$), 2925 (C-H), 2222 (CN), 1464 (CO), 1630 (C=C), 1257 (C-S); ^{1}H NMR (DMSO-d_6, 400 MHz), δ (ppm): 8.67 (s, 1H), 8.26 (d, 1H, ArH), 7.37-739 (m, 3H, ArH), 7.94 (d, 1H, ArH). Elemental analysis: Calculated (%) for $C_{18}H_{12}N_2OS$ (304.37): C, 71.0; H, 3.9; N, 9.2. Found: C, 71.3; H, 3.8; N, 9.4.

2-Amino-4-(pridyl)-4H-chromene-3-carbonitrile (4h): Brown solid, FT-IR (KBr, ν_{max}, cm^{-1}): 3440 (NH$_2$), 2204 (CN), 1472 (CO) 2881 (C-H); ^{1}H NMR (DMSO-d_6, 400 MHz), δ (ppm): 8.6 (s, 1H), 7.1-7.33 (t, 8 H, 1H), 7.8 (d, 1H, ArH) Elemental analysis: Calculated (%) for $C_{19}H_{13}N_3O$ (299.32): C, 76.23; H, 4.3; N, 14.0. Found: C, 75.32; H, 4.24; N, 13.46.

2-Amino-4-(furfuryl)-4H-chromene-3-carbonitrile (4i): FT-IR (KBr, ν_{max}, cm^{-1}): 3457 (NH$_2$), 2227 (CN), 1606 (C=C), 1455 (CO), 1070 (C-C) ^{1}H NMR (DMSO-d_6, 400 MHz), δ (ppm): 9.7 (s, 1H), 7.54-7.51 (t, 8 H, 1H), 7.27–7.23 (m, 3H); Elemental analysis: Calculated (%) for $C_{18}H_{12}N_2O_2$ (288.30): C, 74.99; H, 4.1; N, 9.7. Found: C, 74.32; H, 4.2; N, 8.46.

2-Amino-4-(5-bromo-2-hydroxyphenyl)-4H-chromene-3-carbonitrile (4j): Yellow solid, FT-IR (KBr, ν_{max}, cm^{-1}): 3460 (NH$_2$), 2189 (CN), 1479 (CO), 2883 (C-H), 595 (C-Br); ^{1}H NMR (DMSO-d_6, 400 MHz): 8.3 (s, 1H), 7.29-7.25 (t, 8H, 1H), 7.59–7.56 (m, 3H); ^{13}C NMR (100 MHz) 32.3, 37.1, 48.9, 115.5, 116.3, 117.2, 119.3, 124.2, 125.4, 128.7, 129.5134.1, 135.4, 146.9, 153.4, 160.3, 163.4 Elemental analysis: Calculated (%) for $C_{20}H_{13}N_2O_2Br$ (392.30): C, 61.08.; H, 3.33; N, 7.12. Found: C, 60.72; H, 3.2; N, 7.16.

Recycling of the catalyst: The reusability study on the catalyst is done by taking the condensation reaction of benzaldehyde, malononitrile and β-naphthol, as a model reaction for the recovery investigations. The catalyst is recovered three times by simple filtration and washed with acetone, dried in an oven each time. The results are summarized in Table-5.

The catalytic activity of the catalyst is almost the same as that of freshly used.

Antimicrobial evaluation: The synthesized chromene derivatives (4a-j) are studied for microbial inhibition by Kirby-Bauer disc diffusion method.

TABLE-5
REUSABILITY OF NiO NANOPARTICLES

Run	Time (h)	Yield (%)
1	1	98
2	1	96
3	1	93

The drug amikacin is used as a positive control for antibacterial activity and Flucanazole as a positive control drug for antifungal activity (Table-6).

As seen from the data present in Table-6, it is evident that among all the compounds (4b, 4c, 4d, 4i and 4j) show modest inhibition whereas other compounds have either poor inhibitory activity or do not show any inhibition. Interestingly, compound 4g is the most potent for the inhibition of *Klebsiella pneumonia*. Moreover, it is also evident that among all the compounds (4b, 4c, 4i and 4j) show fungus inhibition whereas other compounds do not show any inhibition.

Protein docking: The chromene ring is an important pharmacophore in modern drug discovery. The knowledge gained by various researchers has suggested that substituted chromenes which interact easily with the receptors and possess different pharmacological activities with lower toxicity. In this study, we identify it *via* docking and their relative stabilities are evaluated, using free energy simulations. Fig. 5 shows the synthesized ligands used for docking.

It is observed that among all the designed compounds, the compound 4f shows better binding nature, which resulted in a decrease in the energy value [39] and also the compound 4j. These compounds show a decreased energy values (-8.55), (-8.32) which means that these compounds are more compatible with the receptor than other designed chromene derivatives and fit well in the receptor cavity forming energetically most stable drug receptor complex. The energy values are calculated and given in Table-7.

Conclusion

In the present investigation, a search of a new source for the production of NiO nanoparticles is successfully carried out. We have developed an efficient and green approach for the one pot three components synthesis of chromenes using NiO nanoparticles as a biodegradable, inexpensive and reusable catalyst. The salient features of our methodology are simple workup, devoid of toxic chemicals, less time consuming, high yield products, easy isolation and also an agreement with the overarching principles of green chemistry. We have utilized the water extract of *Andrographis paniculata,* the natural and low-cost biomaterial for the synthesis of NiO nanoparticles. The components in the water extract serve as reducing, capping and stabilizing agents for nanoparticle generation. FTIR analysis evidences the organic groups involved in the bioconversion of NiO nanoparticles. The EDAX spectrum analysis confirms the generation of NiO nanoparticles. The XRD and SEM analysis

TABLE-6
ANTIBACTERIAL AND ANTIFUNGAL ACTIVITIES OF SYNTHESIZED 2-AMINO-4H-CHROMENES

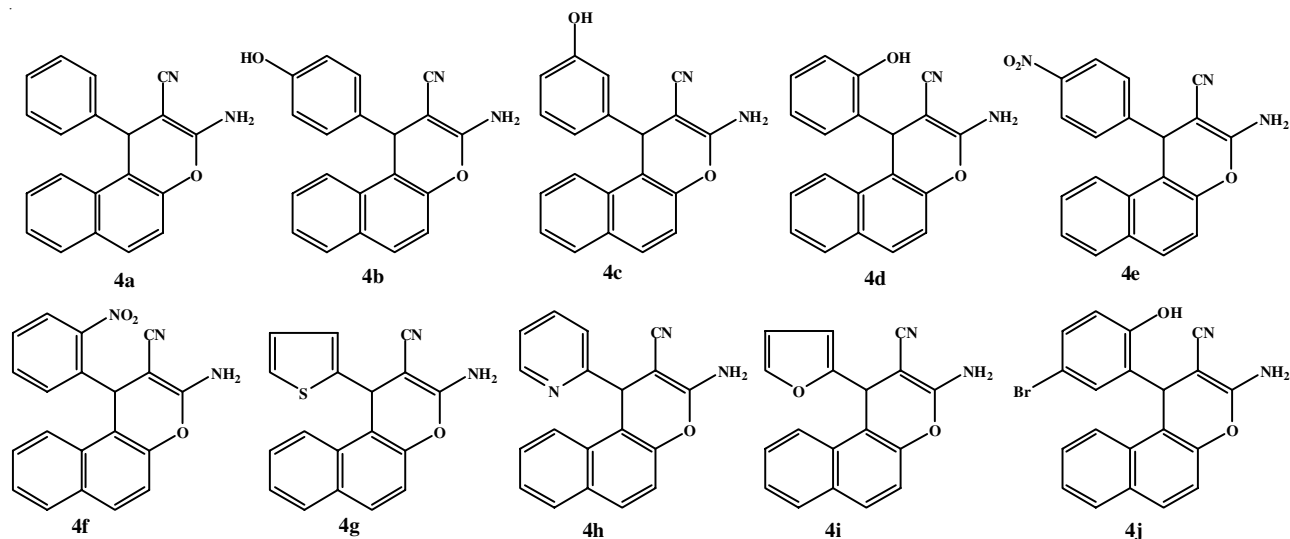| Bacteria/Fungus	4a	4b	4c	4d	4e	4f	4g	4h	4i	4j	Control (mm)
Antibacterial											
Escherichia coli	9	11	11	14	18	9	–	–	20	13	21
Klebsiella pneumonia	10	15	16	14	16	11	32	20	16	12	32
Pseudomonas aeruginosa	9	10	11	11	–	8	–	–	–	–	20
Proteus mirabilis	9	8	16	12	12	13	11	–	11	13	27
Staphylococcus aureus	–	11	17	14	–	–	24	–	18	15	23
Antifungal											
Candida albicans	10	12	17	18	10	17	10	17	28	16	24
Aspergillus oryzae	–	15	25	–	–	–	–	–	27	16	28

Fig. 5. Structure of synthesized ligands used for docking

TABLE-7
DOCKING RESULTS OF SYNTHESIZED 2-AMINO-4*H*-CHROMENES

Compound docked	Binding energy (Kcal/mol)	Types and number of interactions	Residues involved
4a	-8.27	π-sulfur-1 π-π stacked-1 Amide-π stacked -2 Hydrogen bond-1 π-alkyl-1 van der Walls-1 Carbon hydrogen bond	MET A:161 PHE A:149 ALA A:191, PHE A:149 ILE A:194 MET A:147 MET A 232 PRO A 193
4b	-7.83	π-π stacked-1 Amide-π stacked -1 Hydrogen bond-1 π-alkyl-1 van der Walls-1 Carbon hydrogen bond	PHE A:149 ALA A:191 ILE A:194 MET A:147 GLY A:192 PRO A 193
4c	-7.93	π-π stacked-1 Amide-π stacked -1 Hydrogen bond-1 π-alkyl-2 van der Walls-1	PHE A:149 ALA A:191 ILE A:194 MET A:147, ILEA: 202 GLY A:192
4d	-7.62	π-π stacked-1 Hydrogen bond-1 π-alkyl-1 van der Walls-1	PHE A:149 ILE A:194 MET A:199 GLY A:192
4e	-8.08	π-sulfur-1 π-π stacked-1 Amide-π stacked -2 Hydrogen bond-1 π-alkyl-1 van der Walls-1 Carbon hydrogen bond	MET A:161 PHE A:149 ALA A:191 ILE A:194 MET A:147 MET A 232 TYR A: 158
4f	-8.55	π-π stacked-1 Hydrogen bond-3 π-alkyl-2 van der Walls-1	PHE A:149 TYR A:158, LYS A:165, MET A:103 ALA A:191, ALA A:198 GLY A:96
4g	-7.80	π-π stacked-1 Amide-π stacked -1 Hydrogen bond-1 π-alkyl-1	PHE A:149 ALA A:191 TYR A:158 MET A:147
4h	-7.83	π-π stacked-1 Amide-π stacked -1 Hydrogen bond-1 π-alkyl-2	PHE A:149 ALA A:191 TYR A:158 MET A:147, ILE A:202

4i	-8.11	π-π stacked-1	PHE A:149
		Amide-π stacked -1	ALA A:191
		Hydrogen bond-2	TYR A:158, ILE A:194
		π-alkyl-1	MET A:161
		van der Walls-1	PRO A:193
4j	-8.32	Hydrogen bond-2	ILE A:194, TYR A:158
		π-alkyl-3	PROA:193, MET A:199, ALA A:191
		van der Walls-1	MEY A 161
		π-σ-1	PHE A:149

support the crystallinity and surface morphology of the biosynthesized nanoparticles. The average crystallite size for the intense peak measured is 8.5 nm from XRD analysis. TEM and SAED analyses confirm the size of prepared NiO nanoparticles. The synthesized compounds are screened for antibacterial activity and it is observed that 2-amino-4-(5-bromo-2-hydroxyphenyl)-4*H*-chromene-3-carbonitrile) shows the modest activity. In molecular docking studies, the docking scores reveal the binding capacity between ligands and InhA enzyme. The inhibition of InhA disrupts the biosynthesis of mycolic acid which is a central constituent of bacterial cell wall. Therefore, compounds **4f**, **4j** are stable and front-line ligands to overcome the drug resistance of *M. tuberculosis* InhA protein.

ACKNOWLEDGEMENTS

CONFLICT OF INTEREST

The authors declare that there is no conflict of interests regarding the publication of this article.

REFERENCES

1. M.M. Khafagy, A.H.F. Abd El-Wahab, F.A. Eid and A.M. El-Agrody, *Farmaco*, **57**, 715 (2002); https://doi.org/10.1016/S0014-827X(02)01263-6.
2. W.P. Smith, L.S. Sollis, D.P. Howes, C.P. Cherry, D.I. Starkey, N.K.J. Cobley, H. Weston, J. Scicinski, A. Merritt, A. Whittington, P. Wyatt, N. Taylor, D. Green, R. Bethell, S. Madar, R.J. Fenton, P.J. Morley, T. Pateman and A. Beresford, *Med. Chem.*, **41**, 787 (1998); https://doi.org/10.1021/jm970374b.
3. K. Hiramoto, A. Nasuhara, K. Michiloshi, T. Kato and K. Kikugawa, *Mutat. Res.*, **395**, 47 (1997); https://doi.org/10.1016/S1383-5718(97)00141-1.
4. G. Bianchi and A. Tava, *Agric. Biol. Chem.*, **51**, 2001 (1987); https://doi.org/10.1080/00021369.1987.10868286.
5. S.J. Mohr, M.A. Chirigos, F.S. Fuhrman and J.W. Pryor, *Cancer Res.*, **35**, 3750 (1975).
6. D.R. Anderson, S. Hegde, E. Reinhard, L. Gomez, W.F. Vernier, L. Lee, S. Liu, A. Sambandam, P.A. Snider and L. Masih, *Bioorg. Med. Chem. Lett.*, **15**, 1587 (2005); https://doi.org/10.1016/j.bmcl.2005.01.067.
7. F. Eiden and F. Denk, *Arch. Pharm.*, **324**, 353 (1991); https://doi.org/10.1002/ardp.19913240606.
8. S. Makarem, A.A. Mohammadi and A.R. Fakhari, *Tetrahedron Lett.*, **49**, 7194 (2008); https://doi.org/10.1016/j.tetlet.2008.10.006.
9. M. Chen, C. Xie and L. Liu, *J. Chem. Eng. Data*, **55**, 5297 (2010); https://doi.org/10.1021/je100344z.
10. A.G.A. Elagamay and F.M.A.A. El-Taweel, *Indian J. Chem.*, **29B**, 885 (1990).
11. M.M. Heravi, B. BagherNejad and H.A. Oskooie, *J. Chin. Chem. Soc. (Taipei)*, **55**, 659 (2008); https://doi.org/10.1002/jccs.200800098.
12. M.M. Heravi, K. Bakhtiari, V. Zadsirjan, F.F. Bamoharram and O.M. Heravi, *Bioorg. Med. Chem. Lett.*, **17**, 4262 (2007); https://doi.org/10.1016/j.bmcl.2007.05.023.
13. N.K. Shah, N.M. Shah, M.P. Patel and R.G. Patel, *J. Chem. Sci.*, **125**, 525 (2013); https://doi.org/10.1007/s12039-013-0421-y.
14. L. Chen, X.J. Huang, Y.Q. Li, M.Y. Zhou and W.J. Zheng, *Monatsh. Chem.*, **140**, 45 (2009); https://doi.org/10.1007/s00706-008-0008-3.
15. F.K. Behbahani and S. Maryam, *J. Korean Chem. Soc.*, **57**, 357 (2013); https://doi.org/10.5012/jkcs.2013.57.3.357.
16. Z. Afsaneh, M. Roghieh, S. Maliheh, K. Sussan, S.E. Ardestani and F. Alireza, *Iran. J. Pharm. Res.*, **12**, 679 (2013).
17. H.M. Al-Matar, K.D. Khalil, H. Meier, H. Kolshorn and M.H. Elnagdi, *ARKIVOC*, 288 (2008); https://doi.org/10.3998/ark.5550190.0009.g27.
18. B. Baghernejad, M.M. Heravi and H.A. Oskooie, *J. Korean Chem. Soc.*, **53**, 631 (2009); https://doi.org/10.5012/jkcs.2009.53.6.631.
19. S.R. Kolla and Y.R. Lee, *Tetrahedron*, **67**, 8271 (2011); https://doi.org/10.1016/j.tet.2011.08.086.
20. D. Kumar, V.B. Reddy, B.G. Mishra, R.K. Rana, M.N. Nadagouda and R.S. Varma, *Tetrahedron*, **63**, 3093 (2007); https://doi.org/10.1016/j.tet.2007.02.019.
21. T.S. Jin, A.Q. Wang, X. Wang, J.S. Zhang and T.S. Li, *Synlett*, 871 (2004); https://doi.org/10.1055/s-2004-820025.
22. R.L. Magar, P.B. Thorat, V.B. Jadhav, S.U. Tekale, S.A. Dake, B.R. Patil and R.P. Pawar, *J. Mol. Catal. Chem.*, **374-375**, 118 (2013); https://doi.org/10.1016/j.molcata.2013.03.022.
23. S. Khaksar, A. Rouhollahpour and S.M. Talesh, *J. Fluor. Chem.*, **141**, 11 (2012); https://doi.org/10.1016/j.jfluchem.2012.05.014.
24. M.P. Surpur, S. Kshirsagar and S.D. Samant, *Tetrahedron Lett.*, **50**, 719 (2009); https://doi.org/10.1016/j.tetlet.2008.11.114.
25. D.S. Raghuvanshi and K.N. Singh, *ARKIVOC*, 305 (2010); https://doi.org/10.3998/ark.5550190.0011.a25.
26. J.M. Khurana, B. Nand and P. Saluja, *Tetrahedron*, **66**, 5637 (2010); https://doi.org/10.1016/j.tet.2010.05.082.
27. A.V.B.K. Borhade, B.K. Uphade and D.R. Tope, *J. Chem. Sci.*, **125**, 583 (2013); https://doi.org/10.1007/s12039-013-0396-8.
28. A.A. Harb, A.M. El-Maghraby and S.A. Metwally, *Coll. Czech. Chem. Commun.*, **57**, 1570 (1992); https://doi.org/10.1135/cccc19921570.
29. B. Mahesh and S. Satish, *World J. Agric. Sci.*, **4**, 839 (2008).
30. K. Soo-Hwan, H.S. Lee, D.S. Ryu, S.J. Choi and D.S. Lee, *Korean J. Microb. Biotechnol.*, **39**, 77 (2011).
31. O. Trott and A.J. Olson, *J. Comput. Chem.*, **31**, 455 (2010).
32. H.T. Zhang, J. Ding and G.M. Chow, *Mater. Res. Bull.*, **44**, 1195 (2009); https://doi.org/10.1016/j.materresbull.2008.09.042.
33. B.S. Siddiqui, F. Afshan, Ghiasuddin, S. Faizi, S.N.H. Naqvi and R.M. Tariq, *Phytochemistry*, **53**, 371 (2000); https://doi.org/10.1016/S0031-9422(99)00548-8.
34. Q. Huang, D. Li, Y. Sun, Y. Lu, X. Su, H. Yang, Y. Wang, W. Wang, N. Shao, J. Hong and C. Chen, *Nanotechnology*, **18**, 105104 (2007); https://doi.org/10.1088/0957-4484/18/10/105104.
35. J. Parekh and S.V. Chanda, *Turk. J. Biol.*, **31**, 53 (2006).
36. D. Mandal, M.E. Bolander, D. Mukhopadhyay, G. Sarkar and P. Mukherjee, *Appl. Microbiol. Biotechnol.*, **69**, 485 (2006); https://doi.org/10.1007/s00253-005-0179-3.
37. X.-S. Wang, G.-S. Yang and G. Zhao, *Tetrahedron*, **19**, 709 (2008); https://doi.org/10.1016/j.tetasy.2008.02.018.
38. A.F. Latif, *Indian J. Chem.*, **29B**, 664 (1990).
39. R. Siva Kumar, P. Kumarnallasivan, P.R. Vijai Anand, R. Pradeepchandran, K.N. Jayaveera and R. Venkatnarayanan, *Der Pharm. Chem.*, **2**, 100 (2010).
40. T. Clarina, G.R. Priya Dharsini and V. Rama, *Chem. Sci. Trans.*, **6**, 523 (2017); https://doi.org/10.7598/cst2017.1413.